

**WHAT MAKES A LAYER? INVESTIGATING VARIABLE LAYER BEHAVIOR IN MARTIAN NORTH POLAR LAYERED DEPOSITS USING SHARAD MULTIBAND DATA.** Erica R. Jawin<sup>1</sup>, B.A. Campbell<sup>1</sup>, J.L. Whitten<sup>2</sup>, and G.A. Morgan<sup>3</sup> <sup>1</sup>National Air and Space Museum, Smithsonian Institution, Washington, DC ([jawine@si.edu](mailto:jawine@si.edu)). <sup>2</sup>Tulane University, New Orleans, LA. <sup>3</sup>Planetary Science Institute, Tucson, AZ.

**Introduction:** The martian north polar layered deposits (NPLD) are composed of stacks of finely layered ice and dust that form a deposit several kilometers thick, revealed by radar sounding data from the Shallow Radar (SHARAD) on MRO [1, 2]. The ice and dust deposits are the result of cyclic climatic excursions over the past few million years driven by orbital parameter variations, which have led to the repeated deposition and removal of material [1, 3, 4]. Reflectors present in SHARAD radargrams correspond to dielectric interfaces at layer boundaries, which have proven critical to determining the structure of the NPLD and interpreting its evolution [e.g., 1]. However, analyses of SHARAD multiband data in Gemina Lingula found variations in reflector brightness in different frequency subbands, and certain reflectors that only appear in the high- or low-frequency echoes [5]. They argue that resonant scattering within a single SHARAD vertical range cell could give rise to the variable behavior in the SHARAD subbands.

We investigate further the variable reflector behavior in multiband data, and the potential physical implications of this behavior. To do this, we documented the lateral extent and scattering characteristics of a single reflector across ~40 SHARAD radargrams over Gemina Lingula in the NPLD (**Fig. 1A**). We also developed a 1D layer resonance model to investigate how interference between layers of different thickness and spacing could give rise to variations in brightness in the two subbands.

Investigating resonant scattering behavior in NPLD reflectors, and determining the physical configuration of ice/dust layers that give rise to this behavior, is critical to understanding the structure of the polar deposits on Mars—and by extension the climatic evolution. Variations in the brightness, spacing, and number of reflectors in SHARAD radargrams have been used to calculate ice and dust quantities in the polar deposits and used as evidence to constrain climatic evolution [e.g., 6, 7]. However, we find that resonant behavior could

lead to over- or under-estimating layer thickness or brightness, which would affect ice and dust estimates. Deconstructing resonant behavior is also necessary to fully constrain Martian climatic cycles. Understanding resonant behavior in icy target materials using ground penetrating radar data is also important for the upcoming radar sounders RIME and REASON investigating the Galilean satellites.

**Data:** SHARAD transmits a 10-MHz pulse centered at 20 MHz (spanning 15 to 25 MHz), with a free-space range (vertical) resolution of 15 m [8]. This

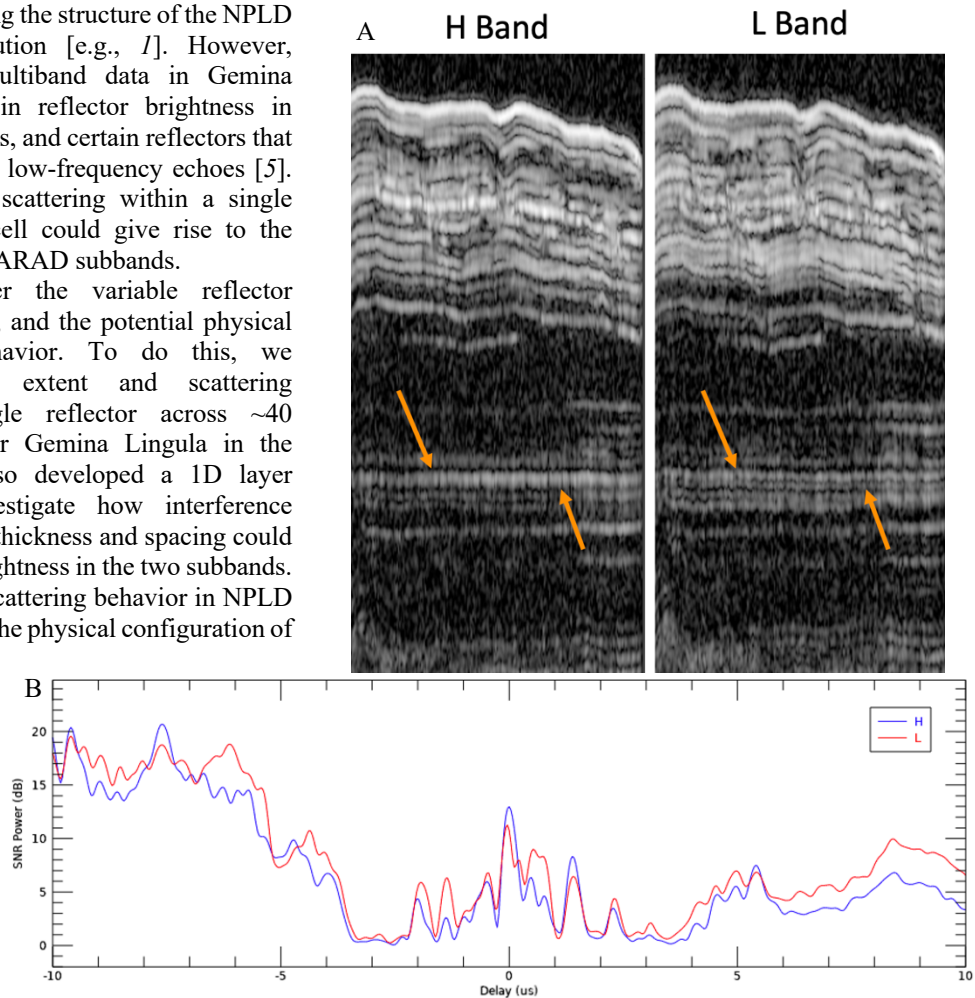


**Fig. 1.** (A) Portion of SHARAD track 13194\_01 over Gemina Lingula shows a single thick reflector in the high-frequency subband (arrows, left) which splits into two thin reflectors in the low-frequency subband (right). (B) Plot showing depth-averaged power. Bands are aligned at the reflector indicated in (A) at 0  $\mu$ s delay. Note the single peak in power for the H band (blue) at 0  $\mu$ s delay compared to the two smaller peaks in the L band (red).

resolution is modulated by dielectric constant by  $1/\sqrt{\epsilon}$ , so the range resolution in water ice with a dielectric constant of 3.12 is 8.5 m. The SHARAD signal can be split into multiple bands across the 10 MHz bandwidth. We use two subbands for our analysis, “high” (center  $\lambda = 13.3$  m, 22.5 MHz) and “low” (center  $\lambda = 17.1$  m, 17.5 MHz) [5]. One radargram is produced for each subband so that differences in scattering behavior of reflectors can be compared between both bands.

To constrain potential layer configurations, we implemented a simple 1D layer resonance model which adds echoes in-phase for up to three layers of dust ( $\epsilon = 4.5$ ) separated by layers of ice ( $\epsilon = 3.2$ ). Each layer has a thickness between 0.1 – 1.0 m, and distance between layers of 0.1 – 3.0 m. This means that the entire stack cannot exceed 9 m, the depth of a single range cell in ice. The round-trip phase is calculated for a large number of random thicknesses and spacings, and the phases of all reflections are added allowing interference between reflections. The resulting output is a histogram of the power ratio (in dB) between the H and L bands.

**SHARAD Behavior:** Our analysis focuses on a distinct reflector in track 13194 in Gemina Lingula which appears as a single bright, thick reflector in the H band, but splits into two thinner, dimmer reflectors in the L band (**Fig. 1**). The reflector is ~2-4 dB brighter in H than in the two layers in the L band (**Fig. 1B**). This behavior spans the entire portion of the SHARAD track crossing Gemina Lingula, ~140 km in length. Within the NPLD, the reflector is part of Unit F [2], or packet 2 [1]. Analyses of other tracks in the region around 13194 show similar behavior—one thick, bright reflector switching to two thinner, dimmer reflectors—in different subbands. However, approximately half the tracks we analyzed show reverse behavior from 13194—the thick, bright reflector is in the L band, splitting into two thinner reflectors in H. Somewhat arbitrarily we refer to the behavior in 13194 as “Type 1”, and the opposite as “Type 2” behavior.

We identified reflectors in 36 tracks with Type 1 or Type 2 behavior located at approximately the same vertical position in Unit F, which we are confident correspond to the lateral extent of the reflector in 13194. The spatial extent of this reflector is widespread, over 300 km, and covers a region over 43,000 km<sup>2</sup> (**Fig. 2**). Of the 36 tracks in this region, 27 (75%) exhibit Type 1 behavior, and 23 (64%) show Type 2 behavior. Many have both Type 1 and Type 2 behavior in different portions of the same track.

**1D Layer Resonance Model Results:** Preliminary results from our modeling suggest that two-layer configurations can readily (i.e., not requiring overly

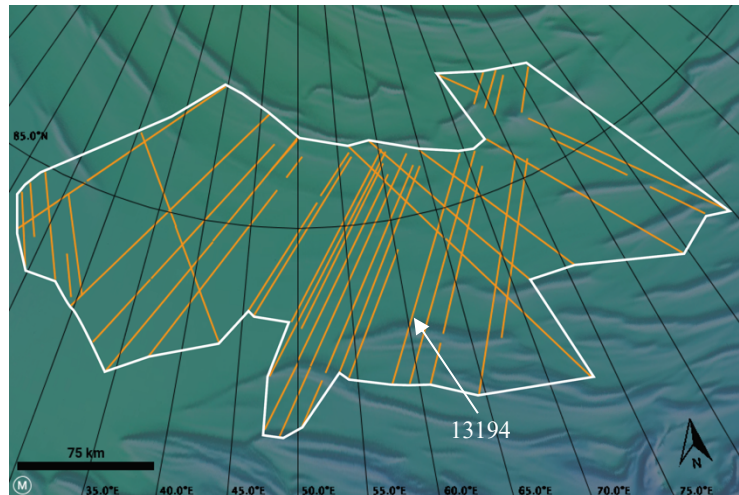


Fig. 2. Portions of SHARAD tracks showing the extent of the Type 1 (Fig. 1) or Type 2 resonant reflector patterns.

strict thickness and spacing) give rise to bimodal behavior, where returned power in the H band is much stronger than the L band (by ~8 dB, corresponding to Type 1), or vice versa (L stronger than H by ~4 dB, corresponding to Type 2). Simulations of one and three layers do not show the same strong behavior favoring one band over the other within the range of thickness and spacing we chose, and instead have unimodal distributions centered on H/L ~ 1. We explored the effects of layer thickness and spacing, and found that the strongest statistical separation of H/L and L/H peaks in the distributions occur in dust layers 10 – 50 cm thick, separated by 0.5 – 3.0 m of ice.

**Implications:** The lateral continuity across Gemina Lingula implies similar depositional conditions over a region comprising tens of thousands of square kilometers. Initial modeling results suggest this reflector can be explained by two thin layers of dust tens of cm thick, separated by up to a few meters ice. This interpretation is consistent with previous observations from HiRISE data [9]. Across the region shown in **Fig. 2** we expect there are subtle variations in layer thickness and/or spacing, which could explain the “flipping” between Type 1 and Type 2 resonant behaviors. It may actually be uncommon to find layers characterized by a simple H/L~1 behavior if there is sub-range resolution layering throughout the NPLD.

**References:** [1] Phillips et al. (2008) *Science*, **317**, 5845. [2] Putzig et al. (2009) *Icarus*, **204**, 443–457. [3] Levrard et al. (2007) *JGR*, **112**. [4] Smith & Holt (2010) *Nature*, **465**, 450–453. [5] Campbell & Morgan (2018) *GRL*, **45**, 1759–1766. [6] Smith et al. (2016) *Science*, **352**, 1075–1078. [7] Lalic et al. (2019) *JGR*, **124**, 1690–1703. [8] Seu et al. (2004) *PSS*, **52**, 157–166. [9] Herkenhoff et al. (2007) *Science*, **320**, 1182–1185.